European Polymer Journal 178 (2022) 111489

Contents lists available at ScienceDirect

European Polymer Journal

journal homepage: www.elsevier.com/locate/europolj

Photocurable extended vanillin-based resin for mechanically and chemically recyclable, self-healable and digital light processing 3D printable thermosets

Anna Liguori [a], Sathiyaraj Subramaniyan [a,b], Jenevieve G. Yao [a], Minna Hakkarainen [a,b,*]

[a] KTH Royal Institute of Technology, Department of Fibre and Polymer Technology, Teknikringen 58, 100 44 Stockholm, Sweden
[b] KTH Royal Institute of Technology, Wallenberg Wood Science Center (WWSC), Teknikringen 58, 100 44 Stockholm, Sweden

ARTICLE INFO

Keywords:
Imine chemistry
Vanillin
Photopolymerization
Recyclable thermoset
Self-healing
Digital light processing 3D printing

ABSTRACT

A vanillin-based photocurable resin was designed for circularity by incorporation of imine functionalities through a Schiff-base reaction between the aldehyde function of vanillin and amino group of ethylene diamine. Sufficient flexibility was provided by a short aliphatic segment introduced by reaction of vanillin with ethylene carbonate, while photocurability was obtained by subsequent methacrylation. The cured thermoset had good solvent resistance, relatively high glass transition temperature (~75 °C) and good thermal stability with an onset of degradation above 300 °C. Due to the crosslinked structure and imine linkages, the thermoset expressed malleability, self-healing and thermal reprocessability. Furthermore, it could be chemically recycled by immersing in ethylene diamine, which activated transimination. The obtained oligomeric product with amine-terminal groups could be utilized for production of new thermoset films. Tensile testing illustrated similar elastic modulus for mechanically and chemically recycled thermosets, while a slight increase was observed for the self-healed samples, ascribable to a completion of the curing during the post-processing. At the same time elongation and stress at break slightly decreased. Finally, the suitability of the resin for the production of 3D objects by means of digital light processing (DLP) 3D printing was demonstrated.

1. Introduction

Traditional thermosets do not fit the circular bioeconomy due to fossil-based origin and difficult recyclability, in best case leading to downcycling. More commonly thermosets are landfilled or incinerated. Utilization of dynamic covalent chemistry (DCC) for production of covalent adaptable networks (CAN) is one of the most attractive approaches for design of circular thermosets [1–4]. These DCC bonds are able to open and reform under the action of a specific stimulus [5–8]. One attractive example is Schiff-base or imine linkages that have ability to participate in both associative, i.e. transimination and metathesis, and dissociative, i.e. hydrolysis, pathways [9,10]. This can be utilized for the development of inedited resins, suitable for the realization of bio-based thermosets endowed with malleability, self-healing and chemical and mechanical recyclability [9,11–19].

Among the biobased molecules, vanillin, produced at industrial scale from lignin [20–22], has risen great interest due to its monoaromatic phenol and aldehyde functions, making this molecule a suitable building block for the preparation of rigid polymers and thermosets with imine-linkages [23–28]. The combination of vanillin-based building blocks and dynamic imine chemistry has been widely reported in literature in particular for the design of monomers, which, thanks to the presence of epoxy functions [29–33] or through condensation reactions [34–38], could be thermally cured leading to the formation of thermosets. Recently, two distinct vanillin-based photocurable vinyl ester resins containing both vinyl and imine bonds were designed [39]. The photocuring process is acknowledged to be particularly suitable for the synthesis of sustainable thermosets, thanks to the low energy requirements, low operational temperature and high efficiency [40–42]. The two resins were obtained from a double step reaction: the methacrylation of vanillin, in order to promote the introduction of vinyl group in the vanillin unit, and the Schiff-base reaction to induce the formation of the imine bonds. The differences between the two resins were related to the amine units employed for the Schiff-base reaction; indeed, both a diamine and a triamine with molecular weights of 148 and 440 g/mol, respectively, were tested. The results clearly

* Corresponding author.
E-mail address: minna@kth.se (M. Hakkarainen).

https://doi.org/10.1016/j.eurpolymj.2022.111489
Received 6 July 2022; Received in revised form 1 August 2022; Accepted 7 August 2022
Available online 17 August 2022

documented the influence of di-or tri-functionality and molecular weight of the amine used. However, the glass transition temperatures of the obtained thermosets were relatively low due to the flexibility of the di-and tri-amine utilized.

In the framework of the development of bio-based, recyclable and thermally stable thermosets, we propose the design of photocurable resins by coupling a vanillin block, properly endowed with vinyl function, and ethylenediamine (molecular weight of 60.1 g/mol). By introduction of a short diamine in the resin structure we aimed to avoid long flexible aliphatic segments, which should increase the glass transition temperature of the resulting thermosets compared to those reported previously [39]. Furthermore, the influence of chemical structure, especially the balance between aromatic/short aliphatic units was investigated by preparing resins based on vanillin and vanillin modified by a short OH-terminated aliphatic chain (extended vanillin). We envisioned that the imine bonds would endow the thermosets with self-healability, mechanical reprocessability and chemical recyclability. At the same time the vinyl functionalities would enable green photocuring and potential 3D printability to tridimensional objects by digital light processing (DLP).

2. Experimental part

2.1. Materials

Vanillin (V) (99 %), ethylene carbonate (EC) (98 %), potassium carbonate (K_2CO_3) (≥99 %), methacrylic anhydride (MAA) (94 %), ethylenediamine (ED) (≥99 %), sodium sulfate (≥99 %), phenylbis (2,4,6-trimethylbenzoyl)phosphine oxide (BAPO) (97 %), *N,N*-dimethylformamide (DMF) (≥99 %), tetrahydrofuran (THF) (≥99 %), and hydrochloric acid (HCl) (37 %) were purchased from Sigma-Aldrich and used without any additional purification. 4-(dimethylamino)pyridine (DMAP) (≥99.0 %, Fluka), sodium bicarbonate (≥99 %, Merck), sodium hydroxide (NaOH) (≥99 %, Fisher Scientific), ethyl acetate (EtOAc) (≥99 %, VWR), dichloromethane (DCM) (≥99 %, Fisher Scientific), ethanol (EtOH) (99.8 %, VWR), acetone (≥99.5 %, VWR) were all used as received.

2.2. Synthesis of extended vanillin (ExtV)

A solution of V (10 g, 65.72 mmol), EC (6.38 g, 72.45 mmol) and K_2CO_3 (11 g, 79.59 mmol) in 100 mL of DMF was added to a 250 mL round-bottom flask with a magnetic stir bar. The reaction mixture was refluxed at 110 °C for 12 h under N_2 atmosphere and the completion of the reaction was verified on TLC plate. Afterwards, the reaction flask was cooled down to room temperature and the reaction mixture was first diluted in distilled water (150 mL) and then poured in EtOAc (150 mL). The aqueous phase was separated and extracted with EtOAc (2x100 mL); the organic phases were mixed, washed with water (2x200 mL), dried over sodium sulfate, concentrated under reduced pressure and further dried in vacuum oven at 60 °C for 12 h, yielding ExtV (white powder, 70 % yield).

^{1}H NMR (400.13 MHz, DMSO- d6): δ ppm 9.84 (s, 1H, –CHO), 7.54 (d, 1H, Ar), 7.40 (s, 1H, Ar), 7.19 (d, 1H), 4.96 (t, 1H, –OH), 4.11 (t, 2H, $–OCH_2CH_2OH$), 3.84 (s, 3H, $–OCH_3$), 3.74–3.78 (m, 2H, $–OCH_2CH_2OH$).

2.3. General procedure for the synthesis of methacrylated vanillin (MV) and methacrylated extended vanillin (M-ExtV)

MV was synthesized according to previously reported procedure [39,43]. Briefly, V (10.13 g, 66.58 mmol), MAA (11.30 g, 73.30 mmol) and DMAP (0.056 g, 0.46 mmol) were added to a 250 mL round-bottom flask with a magnetic stir bar, under reflux and N_2 flow. The reaction was carried out at 60 °C for 24 h. The product of the reaction was diluted with DCM (150 mL) and consequentially washed with saturated aqueous solution of sodium bicarbonate (2x150 mL), 0.5 M NaOH (2x150 mL), 1 M NaOH (150 mL), distilled water (150 mL). The organic phase was dried over sodium sulfate, concentrated at reduced pressure and dried under vacuum at 30 °C for two days, yielding MV (white powder, 75 % yield).

^{1}H NMR (400.13 MHz, DMSO- d6): δ ppm 9.99 (s, 1H, –CHO), 7.63–7.59 (m, 2H, Ar), 7.43 (d, 1H, Ar), 6.31 (s, 1H, -C = CH_2), 5.95 (t, 1H, -C = CH_2), 3.87 (s, 3H, $–OCH_3$), 2.01 (s, 3H, -C-CH_3).

M-ExtV was obtained with a similar procedure. ExtV (5.00 g, 25.51 mmol), MAA (4.29 g, 27.83 mmol) and DMAP (0.019 g, 0.16 mmol) were mixed together in a 50 mL round-bottom flask, under reflux and N_2 flow. The reaction was performed at 60 °C for 24 h and the resulting product was subjected to the same washing procedure used for MV, yielding M-ExtV (pale yellowish powder, 85 % yield).

^{1}H NMR (400.13 MHz, DMSO- d6): δ ppm 9.85 (s, 1H, –CHO), 7.56–7.54 (m, 1H, Ar), 7.42 (d, 1H, Ar), 7.23 (d, 1H, Ar), 6.03 (s, 1H, -C = CH_2), 5.70 (t, 1H, -C = CH_2), 4.47–4.43 (m, 2H, $–OCH_2CH_2OH$), 4.40–4.36 (m, 2H, $–OCH_2CH_2OH$), 3.84 (s, 3H, $–OCH_3$), 1.88 (s, 3H, -C-CH_3).

2.4. General procedure for the synthesis of Schiff-base resins

Two Schiff-base resins, SB1 and SB2, were obtained by imination of MV and M-ExtV, respectively, with ED. Briefly, solutions of MV (3.00 g, 13.62 mmol) or M-ExtV (3.60 g, 13.62 mmol), and ED (0.41 g, 6.82 mmol) in 50 mL of DCM were added to a 150 mL round-bottom flask and kept under stirring in environmental conditions for 5 h. The collected reaction mixtures were washed according with the procedure described for the methacrylation reactions, and named SB1 (yellowish powder, 81 % yield) and SB2 (white powder, 82 % yield), respectively.

SB1 ^{1}H NMR (400.13 MHz, DMSO- d6): δ ppm 8.36 (s, 2H, –HCN-), 7.50 (d, 2H, Ar), 7.34–7.30 (m, 2H, Ar), 7.21 (d, 2H, Ar), 6.28 (s, 2H, -C = CH_2), 5.91 (t, 2H, -C = CH_2), 3.90 (s, 4H, $–NCH_2CH_2N$-), 3.79 (s, 6H, $–OCH_3$), 1.99 (s, 6H, -C-CH_3). SB2 ^{1}H NMR (400.13 MHz, DMSO- d6): δ ppm 8.25 (s, 2H, –HCN-), 7.35 (d, 2H, Ar), 7.20–7.17 (m, 2H, Ar), 7.04 (d, 2H, Ar), 6.02 (s, 2H, -C = CH_2), 5.69 (t, 2H, -C = CH_2), 4.46–4.39 (m, 4H, $–OCH_2CH_2OH$), 4.39–4.26 (m, 4H, $–OCH_2CH_2OH$), 3.82 (s, 4H, $–NCH_2CH_2N$-), 3.78 (s, 6H, $–OCH_3$), 1.87 (s, 6H, -C-CH_3).

2.5. Photocuring of films of the Schiff-base resins

Photopolymerized thermosets, abbreviated as X-SB1 and X-SB2, were obtained by solubilizing SB1 and SB2, respectively, in DCM with a concentration of 70 % w/v. After the complete solubilization of the resins, BAPO (10 % w/w) was added and stirred for 30 min. The resulting solutions were then poured in Teflon circular (inner diameter: 36 mm) or rectangular (80 (L) × 5 (W) × 0.5 (T) mm) molds and subjected to photocuring for 10 min under the 36 W UV curing lamp with the wavelength of 385 nm and irradiation intensity of 2.6 ± 0.4 mW/cm^2. The resulting films were left under the fume-hood for three days in order to allow the complete evaporation of the DCM.

2.6. Self-healing and mechanical recycling

The self-healing ability of X-SB2 was tested by cutting the specimens in the middle by using scissors; after, the two pieces were partially overlapped and pressed under 1 kg weight at 125 °C for 30 min. Mechanical recycling of X-SB2 was performed by cutting the film in small pieces with help of scissors and of a mortar. The collected fragments were transferred to a square-shaped mold (25 × 25 × 0.5 mm) and hot-pressed at 200 °C for 5 min under 2 MPa.

2.7. Chemical recycling

Chemical recycling of X-SB2 was performed by solubilizing 0.750 g of X-SB2 in 10 mL of ED for 4 h at 60 °C. The resulting product was precipitated in water, subjected to vacuum filtration and dried in

vacuum oven at 60 °C for 72 h. 300 mg of the polymer, 100 mg of M-ExtV and 10 mg of BAPO were pressed together in a mortar and further mixed inside a round-bottom flask with a magnetic stir. The powder was then poured in a square-shaped mold (25 × 25 × 0.5 mm) and hot-pressed at 125 °C for 30 min under 2 MPa. The resulting film was UV cured on both the sides for 10 min/side.

2.8. Digital light processing (DLP) 3D printing

A solution of SB2 monomer (70 % w/v) and BAPO (5 % w/w) in DCM was 3D-printed by using a commercial DLP printer from ASIGA (MAX X, light emission at λ = 385 nm, nominal xy pixel resolution of 27 μm). The UV light intensity, the layer thickness and exposure time were set at 29.69 mW/cm^2, 0.05 mm and 67 s, respectively. After printing, the objects were sonicated in acetone for 15 min to remove the unreacted monomer.

2.9. Characterizations

The ^{1}H nuclear magnetic resonance (NMR) spectroscopy of synthesized ExtV, MV, M-ExtV, SB1 and SB2 was performed on an Avance 400 (Bruker, U.S.A.) spectrometer (400 MHz), using deuterium dimethyl sulfoxide (DMSO) as a solvent for all the samples. The chemical structures of the produced resins and thermosets as well as of the reprocessed samples were investigated by a PerkinElmer Spectrum 2000 Fourier transform infrared (FTIR) spectrometer (Norwalk, CT) equipped with an attenuated total reflectance (ATR) sampling accessory. All the spectra were scanned in the range of 4000–600 cm^{-1} with a resolution of 4 cm^{-1}.

Differential scanning calorimetry (DSC) analysis of X-SB1 and X-SB2 were performed on a METTLER TOLEDO DSC820. Samples with a weight around 5 mg were weighed and sealed into 100 μL aluminum crucibles. All the samples were first cooled to −10 °C and subjected to a heating ramp up to 200 °C with a heating rate of 10 °C/min. Measurements were performed under a nitrogen flow rate of 50 mL/min. Thermogravimetry (TGA) analysis of X-SB1, X-SB2 and reprocessed samples were carried out in a TGA/SDTA851e (METTLER TOLEDO, U.S.A.). Samples with a weight around 10 mg, were inserted in 70 μL ceramic crucibles and subjected to a heating scan from 30 °C to 600 °C with a heating rate of 10 °C/min and under a 50 mL/min nitrogen flow.

Dynamic mechanical analysis (DMA) was performed on all the produced and reprocessed thermosets by using a TA Instruments Q800 in the tension film mode. The experiments, in a multifrequency strain mode, were performed with a force track of 125 % at a frequency of 1.0 Hz. The deflection amplitude of oscillation and Poisson's ratio were set at 15 μm and 0.44, respectively. The samples were equilibrated at 25 °C for 5 min and tested from 25 °C to 190 °C at 1 Hz with an amplitude oscillation of 15 μm and at a 3 °C/min heating rate. The glass transition temperature was considered as the maximum of the tan δ curve and the crosslinking density was estimated according to equation (1).

$$\upsilon = E^{'}/3RT \quad (1)$$

where E' is the storage modulus in the rubbery plateau at the temperature T and R is the universal gas constant (8.314 J/(mol K)). The same instrument was employed to investigate the stress relaxation properties of X-SB2. Measurements were conducted at different temperatures (110 °C, 115 °C, 120 °C, 125 °C and 130 °C). The thermosets were first heated to the desired temperature and equilibrated for 5 min; after that, a constant 1 % strain was applied to the thermosets, and the relaxation modulus and stress were recorded over time. Mechanical properties, i.e. Young's Modulus, stress at break and strain at break, of X-SB2 and of all the reprocessed materials (20 mm × 5 mm × ~ 0.3 mm) were investigated by means of an Instron 5944 universal testing machine. Thickness for each analyzed sample was considered as the mean value of 5 different measurements performed along the specimen's length. All the samples were conditioned at 22 °C and 40 % relative humidity for 2 days before testing.

3. Results and discussion

We successfully designed malleable, reprocessable and chemically recyclable thermosets by utilizing a photopolymerizable vanillin Schiff-base resin. Two resins and the resulting cured thermosets were carefully characterized and the most promising resin was tested for self-healing, and mechanical and chemical recyclability. Furthermore, the suitability for the production of tridimensional objects by means of DLP was demonstrated.

3.1. Synthesis of the resins

The double- and triple-step reaction processes employed for the attainment of SB1 and SB2 resins, respectively, are reported in Fig. 1. For the synthesis of SB1, first the phenolic function of vanillin was subjected to the methacrylation reaction with methacrylic anhydride (2) [39], after which its aldehyde group was involved in the Schiff-base reaction with ED (3). For SB2, a similar procedure was followed except there was an additional step consisting of a nucleophilic substitution reaction between the phenolic group of vanillin and ethylene carbonate (1) in the presence of K_2CO_3. The reaction led to the obtainment of the extended vanillin with a short aliphatic unit terminated with an –OH group (ExtV), which was exploitable for the formation of the ester bond in the follow-up methacrylation reaction.

The chemical structure of all the synthesized molecules was confirmed by ^{1}H NMR analysis (**Figure S1-S5**). The collected spectra documented the successful formation of the ExtV (**Figure S3**), as confirmed by the presence of the peaks at δ 4.11 and δ 3.75 ppm (hydrogens of the aliphatic unit), and of the peak at δ 4.96 ppm (terminal –OH group) [44]. The methacrylation reactions were confirmed for both V (**Figure S1**) and ExtV (**Figure S4**) and they were documented by the appearance of two new signals, ascribable to the introduction of the vinyl functions, at δ 6.31 ppm and δ 5.95 ppm as well as at δ 6.03 and δ 5.70 ppm for MV and M-ExtV, respectively. The follow-up Schiff-base reactions (**Figures S2 and S5**) were documented by the disappearance of the signal at around δ10.0 ppm (aldehyde group) and the appearance of a new signal at around δ8.30 ppm (imine group).

3.2. UV-curing of SB1 and SB2

The influence of the additional short aliphatic unit in the extended vanillin-based monomer, ExtV, was evident after the UV-curing step. Indeed, when SB1 was cured to X-SB1 thermosets, this resulted in fragile and non-uniform films or specimens (Fig. 2**d**). The variation of the conditions, such as the curing time, the concentration of the monomer in DCM and the amount of photo-initiator, did not improve the quality of the thermoset. Differently from SB1, SB2 turned out to be curable to uniform and homogenous films (Fig. 2**b**) and specimens (Fig. 2**c**). The presence of the additional aliphatic unit conferred higher flexibility to the resulting monomer, contributing to the formation of a more flexible crosslinked networks also by increasing the distance among the aromatic rings and the crosslinking points, with a consequent improvement of film forming properties. The successful photopolymerization of both resins was confirmed by ATR-FTIR (Fig. 2**a**), which documented the decrease of the intensities of the absorption bands at 950 cm^{-1} and 865 cm^{-1}, both ascribable to -C═C- bending vibrations, in the cured thermosets with respect to the resins. The absorption bands of imine and carboxyl functionalities remained after the photopolymerization.

3.3. Thermal and solvent resistance of X-SB1 and X-SB2

Both X-SB1 and X-SB2 turned out to be thermally stable, showing the onsets of degradation ($T_{5\%}$, 5 % weight loss) above 300 °C and similar

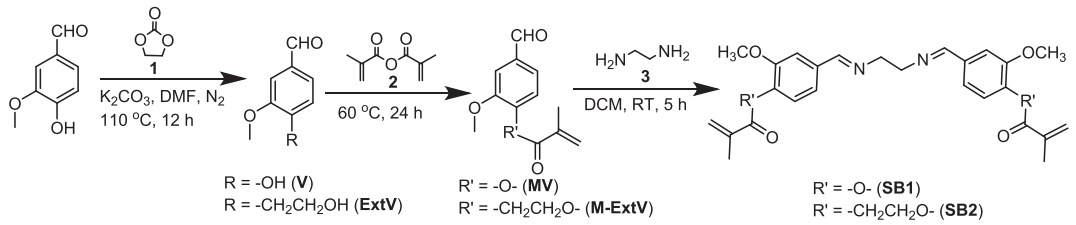

Fig. 1. Scheme of reactions for the synthesis of SB1 and SB2 resins.

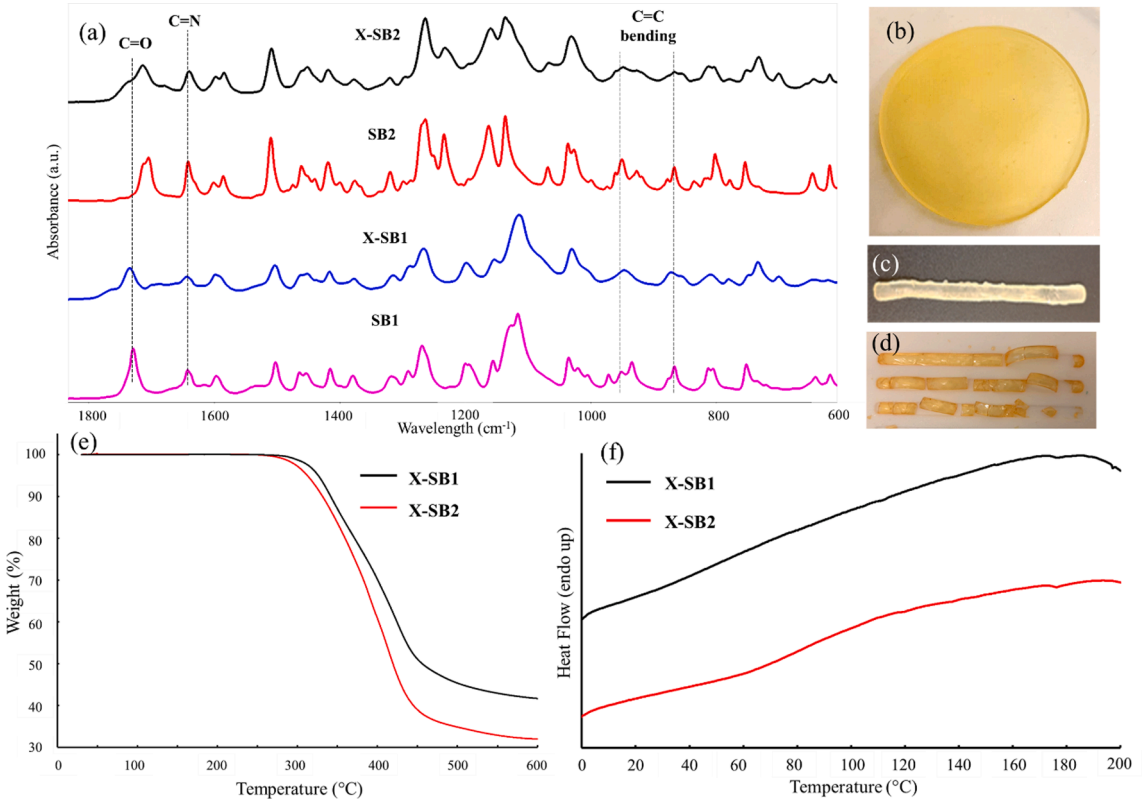

Fig. 2. (a) ATR-FTIR spectra of original resins and cured thermosets; (b) X-SB2 thermoset films; (c) X-SB2 specimen; (d) X-SB1 specimens; (e) TGA curves of X-SB1 and X-SB2, (f) DSC curves of X-SB1 and X-SB2.

maximum degradation temperatures (T_d), as observable in Fig. 2**e** and in Table 1. The slightly lower stability of X-SB2 is ascribed to the presence of the additional aliphatic units, which induced an anticipated decrease of the degradation onset temperature, in tune with previously reported results for other systems [45,46]. Accordingly, a larger residue was found at 600 °C for X-SB1 with respect to X-SB2, due to the higher density of the aromatic units in the network structure.

According to DSC analysis (Fig. 2**f** and Table 1), X-SB1 and X-SB2 were characterized by similar T_g values. These glass transition temperatures turned out to be significantly higher with respect to those reported previously for vanillin thermosets obtained by employing longer diamine (T_g = 31 °C) or triamine (T_g = 25 °C) [39]. Opposite to the previous work the thermosets presented in this work are, thus, in glassy state at room temperature and expected to exhibit higher rigidity. The slightly higher T_g of X-SB2 with respect to X-SB1 could be ascribed to more complete curing reached thanks to the more flexible starting monomer. This is supported by the higher solvent resistant properties of X-SB2 (Table 1). The gel content measurements performed in common solvents, i.e. DCM (Table 1), HCl, DMF, acetone, EtOH, THF (Table S1 and S2), documented good solvent resistance for both thermosets. Furthermore, the stability of X-SB2 was significantly higher compared to X-SB1 in all tested solvents, in tune with the higher curing degree. All the samples preserved their film morphology after 48 h of immersion; although some minor change of color could be observed for both thermosets after immersion in HCl and acetone (**Figure S6**). This phenomenon could be explained by assuming some minor imine bond dissociation taking place in HCl and the occurrence of some imine exchange reactions in acetone. Because continuous thermosets could not be obtained with SB1 resin, the following characterizations are only reported for X-SB2 thermosets.

Table 1
Thermal properties and gel content in DCM of X-SB1 and X-SB2.

Sample	T_g (°C) DSC	DMA	T_5 (°C)	T_d (°C)	Residue at 600 °C	Gel contentDCM (w/w %)
X-SB1	67 ± 3	–	326 ± 1	425 ± 1	40 ± 2 %	81 ± 3
X-SB2	75 ± 2	83 ± 2	311 ± 4	417 ± 3	31 ± 3 %	89 ± 2

3.4. Thermomechanical properties

According to the analysis in multifrequency strain mode (Fig. 3**a**), X-

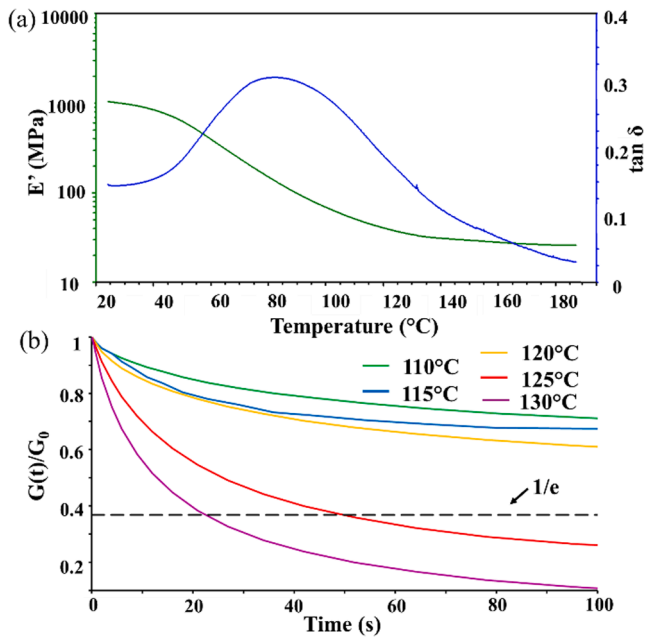

Fig. 3. (a) *E'*(green) and tan δ (blue) curves of X-SB2 as a function of temperature; (b) X-SB2 normalized stress relaxation modulus as a function of time at different temperatures.

SB2 network illustrated a T_g of 83 °C ± 2 °C, as determined from the tan δ curve and as shown in Table 1, and *E'* at 25 °C of 1161 ± 180 MPa. The crosslinking density of (3.7 ± 1.3) × 10^3 mol/m^3 was calculated with eq (1). Moreover, as observable from the representative curve in Fig. 3**a, E'** of X-SB2, after reaching the rubbery plateau, turned out to be stable at temperatures, which were 110 °C higher than T_g. This demonstrates the preservation of the crosslinking density even at higher temperatures. Stress relaxation measurements performed at different temperatures in the range 110 °C-130 °C are reported in Fig. 3**b**. The curves illustrate a decrease of the normalized stress relaxation modulus with the time. However, for the lowest investigated temperatures (110 °C, 115 °C and 120 °C), the relaxation of the stress was not reached. Conversely, the stress relaxation modulus reduced more than 37 % in less than 1 min when the thermoset was subjected to higher temperatures, i.e. 125 °C and 130 °C, highlighting the potential of the material to release the stress. This interesting behavior confirms the rigidity of the structure [9], and the absence of significant imine exchange reactions at temperatures below 125 °C.

3.5. Malleability of X-SB2

The malleability of the produced thermoset was verified through an investigation of its shape-memory behavior. X-SB2 samples were heated on a heating plate at 100 °C for 2 min, in order to confer mobility to the network, without inducing imine activation, as demonstrated by the stress-relaxation tests. As shown in Fig. 4**a**, the samples could be modified in a temporary shape, which was fixed through a fast cooling of the sample performed by immersing in cold water. When subjected to reheating at 100 °C, the samples recovered their initial shape in around 10 s (**Video S1**), demonstrating the malleability of the thermosets. Furthermore, it was also possible to consequently confer different temporary shapes to the same specimen, by heating it above the T_g (Fig. 4**b**). However, when heated, the sample was not able to completely recover its original shape (**Video S2**). The behavior was similar to what previously observed for other Schiff-base thermosets subjected to annealing processes [47]. The failure to completely recover the initial shape can be ascribed to a possible activation of the imine functions, and to the readjustment of the network, occurring as a function of the number of heating steps to which the sample was subjected to. Indeed, in tune with previous research [48], the potential of a thermoset to be formed in a temporary shape is strictly related to its physical phase transitions. For these transitions, temperature is the most relevant parameter. The memory of the original shape, instead, is strictly connected to the remodeling of the molecular structure by dynamic bond exchange, and it is therefore highly dependent on the temperature and time.

3.6. Self-healing and mechanical and chemical recyclability

Due to the presence of the imine functions, the X-SB2 thermoset turned out to exhibit self-healing properties and it was also mechanically reprocessable (Fig. 5**a-c**). To evaluate the self-healing ability, the sample was cut into two pieces and the overlapped specimens were then heated at 125 °C for 30 min to activate the imine exchange. This resulted in a successful welding of the specimens to SH X-SB2. For mechanical recycling by thermal reprocessing, the original thermoset cut into small pieces could be processed into new homogeneous films by hot-pressing at 200 °C for only 5 min (Fig. 5**d**).

The chemical recyclability was demonstrated according to an inedited procedure, summarized in Fig. 5**e**, based on: (i) a transimination pathway initiated by immersing X-SB2 in excess of ED, which lead to the conversion of the thermoset into non-crosslinked recycled oligomeric products (O-SB2), as confirmed by the complete solubilization of X-SB2 in ED (Fig. 5**e**); (ii) the recovery of O-SB2 in the form of powder by precipitating the recycled product in water; (iii) the mixing of O-SB2 powder with M-ExtV and photo-initiator, followed by the hot-press, in order to induce the Schiff-base reaction directly in the solid state, followed by subsequent UV curing of the hot-pressed film. Due to the excess of ED added during the chemical recycling process, the recycled product

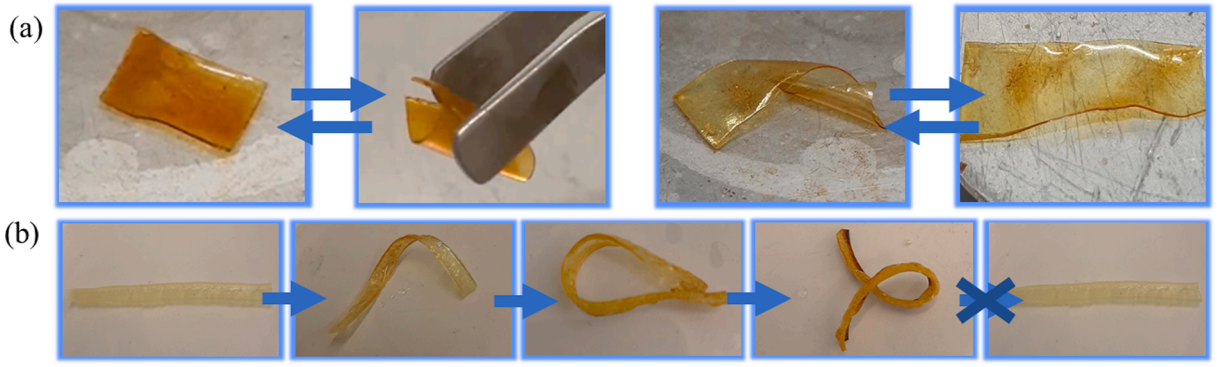

Fig. 4. (a) Reversibility of the passage from the original shape to the temporary shape; (b) Different temporary shapes consequentially conferred to the same specimen.

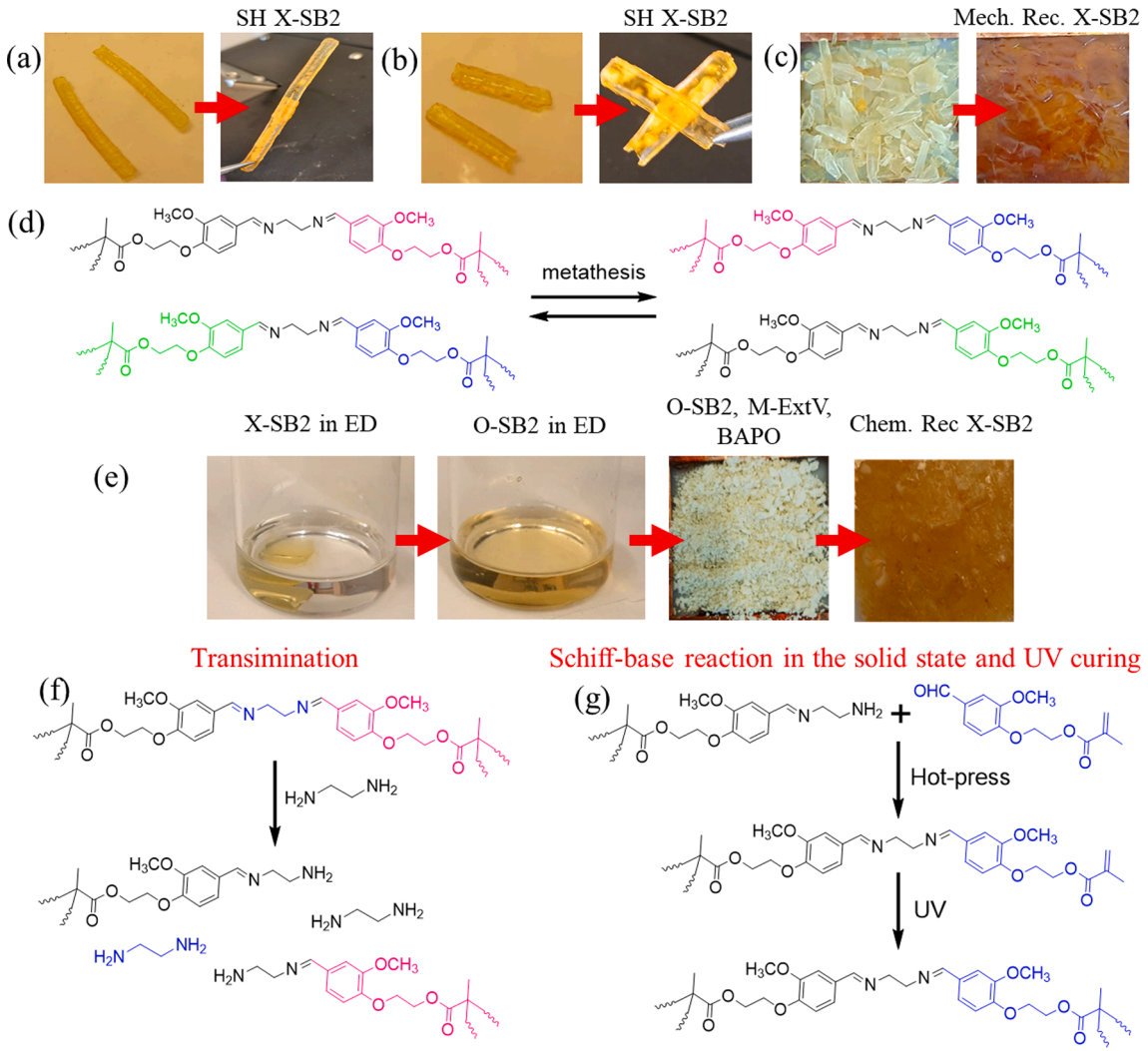

Fig. 5. (a, b) Photo images of the cut sample specimens before and after the self-healing procedure; (c) Mechanical recycling of X-SB2 by reprocessing cut pieces with hot-press; (d) Suggested metathesis pathway leading to the self-healing and mechanical recyclability of X-SB2; (e) Summary of the chemical recycling procedure: photos of X-SB2 immediately after the immersion in ED and after 4 h immersion in ED at 60 °C; photos of recovered powder of O-SB2 mixed with M-ExtV and BAPO photo-initiator before and after the hot-press and subsequent UV curing; (f) Suggested transimination pathway leading to the solubilization of X-SB2 in ED; (g) Suggested reactions occurring during the hot-press and UV curing.

mainly consists of oligomers with amine end-groups. Therefore, to be able to cure the resin again, some new M-ExtV needed to be added to react with these amine-functionalities. The possible transimination pathway, Schiff-base and photopolymerization reactions are schematized in Fig. 5**f and g**.

^{1}H NMR analysis (Fig. 6**a**) was carried out on the solution of O-SB2 in ED and, in tune with the anticipated results, the presence of peaks clearly ascribable to the original SB2 were present in the region between δ 7.00 and δ 7.50 ppm and around δ 3.75 ppm. Due to the occurrence of the transimination pathway, the peak at δ 8.25 ppm of the imine functions was still detectable. The two vinyl peaks (at δ 6.02 and δ 5.69 ppm) of the resin were replaced by a single peak at δ 5.85 ppm. This can be ascribed to the reaction of the carbon double bond during the UV curing reaction for the formation of X-SB2. From the ATR-FTIR analysis performed on collected O-SB2 and shown in Fig. 6**b**, after the precipitation in water and drying, no great differences were observed between the spectrum of collected O-SB2 and the spectrum of X-SB2 (Fig. 1**a**), except for the intense signal centered at 3400 cm^{-1}, suggesting as expected the presence of –NH_2 units in the recycled oligomer, as schematically reported in Fig. 5**f**.

Tensile testing was employed to investigate the mechanical properties of X-SB2 and all the reprocessed samples. The tensile properties are reported in Fig. 7**a** and in Table 2. Moreover, **Figure S7** documented that the breakage of SH X-SB2 specimen during tensile testing did not take place in the area in which the self-healing occurred, in tune with previous results reported for imine-based thermosets [32,49]. The mechanical and the chemical recycling did not induce any significant changes of the elastic modulus, while a slight increase of modulus was observed for the self-healed sample. The strain at break and stress at break were slightly reduced for all reprocessed samples.

ATR-FTIR analysis (Fig. 7**b**) provided a possible explanation for these results. Indeed, from the comparison of the collected spectra, the self-healed and mechanically recycled samples showed an evident modification of the absorption band placed at 948 cm^{-1} with respect to X-SB2, highlighting a possible completion of the curing during the reprocessing. However, a peak at 1680 cm^{-1}, probably ascribable to the reformation of some aldehyde functions, was detected in all the reprocessed samples and it turned out to be clearly evident especially in the mechanically recycled materials, for which a decrease of the intensity of the imine absorption band was also observed. In tune with these considerations, the increase of the Young's modulus registered for SH X-SB2 could be linked to the additional thermal curing, which did not significantly affect the imine bonds. It is worth mentioning that the greatest standard deviation was observed for SH X-SB2 compared with the other samples,

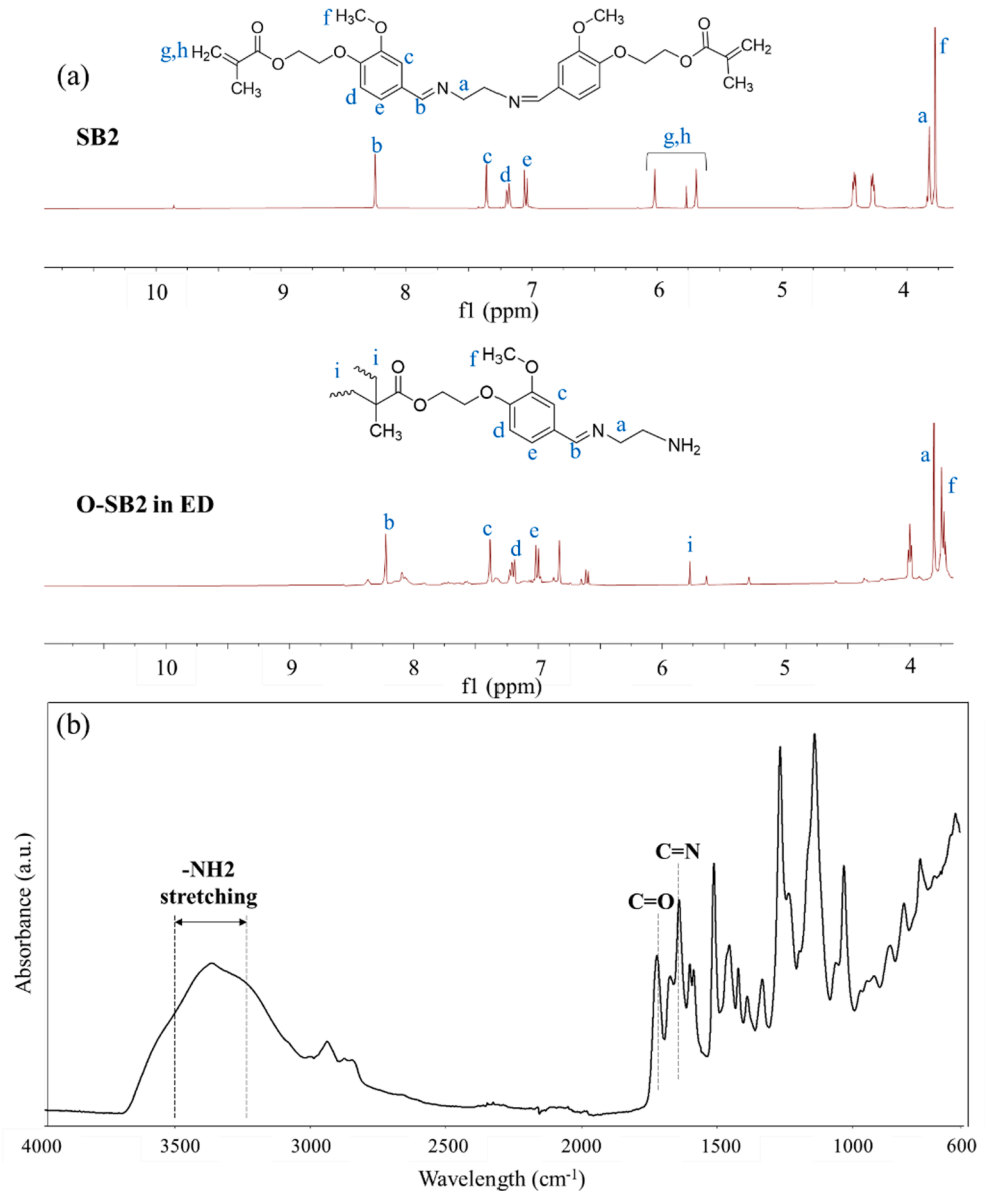

Fig. 6. (a) Comparison of ^{1}H NMR spectra of SB2 (up) and O-SB2 in ED (down); (b) ATR-FTIR spectrum of O-SB2 powder.

likely ascribed to the non-uniform thickness and length, of this kind of samples. Finally, the reduction of the stress and strain at break, registered for all the reprocessed materials in comparison to the X-SB2, could be ascribed to the different manufacturing procedures to which the samples were subjected to, which led to modification of the X-SB2 network structure. In tune with a completion of the curing and the activation of imine bonds at the employed temperature, the additional thermal treatment relevantly decreased the strain at break of the SH samples with respect to the original thermoset, leading to higher rigidity [50]. A comparison of X-SB2 and Mech. Rec. X-SB2 (Table 2), shows that a slight reduction of both the elongation at break and the stress at break were observed for the recycled samples. A possible explanation of the observed phenomenon could lie in the opening of the imine bonds, which was only partially compensated by the completion of the curing, leading to overall decrease of the network's rigidity. Differently from SH X-SB2 and Mech. Rec. X-SB2, for which the thermal treatment can be considered as an additional step to the photocuring, the processing procedure was significantly different for Chem. Rec. X-SB2 and a direct comparison is difficult to be made. The lowest flexibility and stress at break of Chem. Rec. X-SB2 might be explained by considering, respectively, the greater rigidity of the O-SB2 with respect to SB2 and the expected lower density of the imine bonds, formed through a solid-state reaction, in the reprocessed sample.

The reprocessed films were thermally characterized and their solvent resistance properties in DCM were investigated. As observable from TGA analysis (Fig. 7**a**), all the materials turned out to be very stable up to 250 °C. In the temperature range 250 °C-370 °C, a first degradation step was observed only for Mech. Rec. X-SB2. This can be attributed to the lower content of imine bonds, which could also explain the reduced thermal stability in this temperature range with respect to SB2. Between 370 °C and 450 °C, the TGA curves of X-SB2 and all the reprocessed samples appeared very similar each other; while a faster degradation of the monomer, ascribable to the absence of crosslinked structure, can be observed. All the thermosets demonstrated a residue higher than 24 % w/w at 600 °C, with some differences among them probably caused by the different methods employed for their reprocessing.

DMA was employed to determine the effect of reprocessing on T_g. As shown in Fig. 8**b**, no great variations were registered after the reprocessing. Slight shifts towards higher temperatures (104 °C) were registered for self-healed and chemically recycled materials, ascribable in the

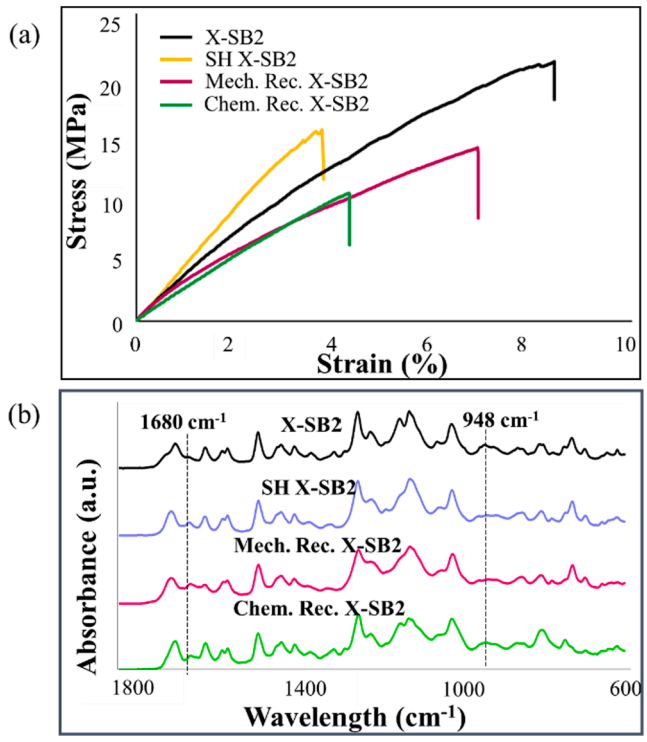

Fig. 7. (a) Representative stress–strain curves of X-SB2 and all reprocessed samples; (b) ATR-FTIR spectra of X-SB2 and all the reprocessed samples.

Table 2
Mechanical properties of X-SB2 and all the reprocessed samples.

Sample	Elongation at break [%]	Stress at break [MPa]	Elastic modulus [MPa]
X-SB2	9.0 ± 1.1	17.3 ± 3.9	370 ± 79
SH X-SB2	3.4 ± 0.7	13.0 ± 2.8	567 ± 103
Mech. Rec. X-SB2	7.5 ± 2.1	11.4 ± 2.4	316 ± 81
Chem. Rec. X-SB2	4.9 ± 1.4	10.3 ± 1.2	342 ± 43

first case to the completion of the curing, and in the second case to the different procedure employed for the reforming of the thermoset. Interestingly, for all the reprocessed samples, narrower curves and, therefore, more defined T_g values were collected. This suggests the presence of a more uniform network in the reprocessed samples with respect to the starting material.

The solvent resistance (gel content) of the reprocessed films was evaluated by immersing them in DCM for 48 h. As observable, the chemically recycled films, Chem. Rec. X-SB showed a gel content (88 ± 2 %) similar to the original X-SB2 (89 ± 2 %); while a slight decrease respective increase of this value was registered for Mech. Rec. X-SB2 (84 ± 3 %) and SH X-SB2 (94 ± 1 %). The slight decrease observed for the mechanically recycled sample is likely due to the opening of some of the imine functions, in tune with the ATR-FTIR and TGA results. On the other hand, the increased stability detected for SH X-SB2 correlates with the completion of the curing and the resulting higher rigidity.

3.7. Digital light processing 3D printing of SB2 resin

SB2 resin was also successfully 3D printed to tridimensional objects by DLP. Fig. 9**a and 9b** illustrate two 3D printed objects, a diamond and a stair, starting from the bio-based resin with dynamic covalent imine bonds. A good printing accuracy was demonstrated (**Figure S8**). The possibility to DLP 3D print bio-based resins was reported by several

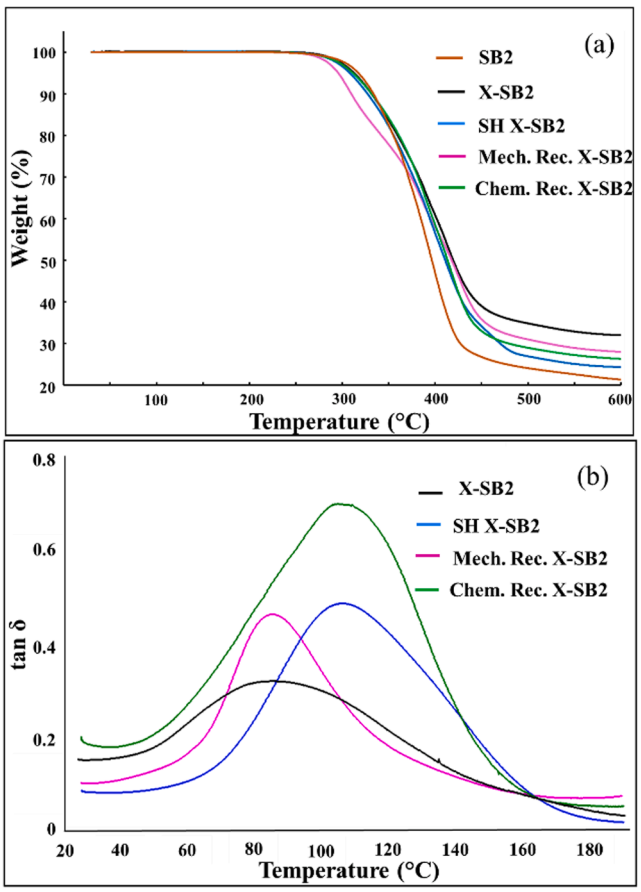

Fig. 8. (a) TGA analysis of X-SB2 and of all the reprocessed samples; (b) tan δ curves obtained from analysis in multifrequency strain mode performed on X-SB2 and the reprocessed samples.

authors [51–53]. However, we only found one previous report of DLP 3D printable resins with imine bonds [54] with a resin based on a fossil fuel-derived monomer.

4. Conclusions

A vanillin-based photocurable resin was successfully designed for circularity by incorporation of imine functionalities. The novel resin was obtained by a Schiff-base reaction between methacrylated extended vanillin and ethylenediamine. The introduction of –OH terminated short aliphatic unit in the vanillin structure (SB2) turned out to be indispensable for the UV curing of the resin into homogeneous and uniform films, while coherent films and specimens could not be produced from the more rigid plain vanillin-based resin (SB1). The UV curing of the vinyl functionalities enabled obtainment of thermosets endowed with high thermal stability (onset of degradation above 300 °C), high solvent resistance properties and malleability. The presence of imine bonds conferred self-healing properties and mechanical recyclability to the thermoset, following a metathesis pathway, which was activated at temperatures higher than 120 °C, as documented by the stress relaxation analysis. Moreover, these bonds also enabled facile chemical recycling of the thermoset, in the presence of an excess of ethylene diamine. The recovered recycled oligomer, could be utilized as a component in new resins that were cured by hot-pressing and subsequent UV-curing. The characterizations carried out on all the reprocessed materials confirmed the preservation of the high elastic modulus, thermal stability and solvent resistance properties. Finally, the synthesized resin was demonstrated suitable for the production of tridimensional objects by means of digital light processing (DLP) 3D printing. Taking together, the results

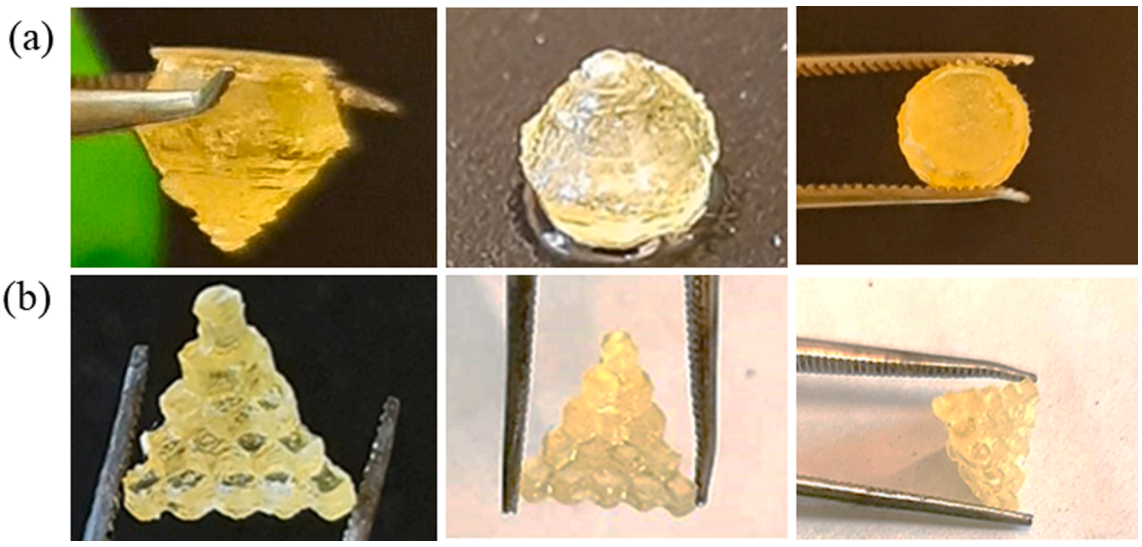

Fig. 9. (a) 3D printed diamond; (b) 3D printed stairs. Both objects were obtained by digital light processing 3D printing of SB2 resin.

documented the possibility to develop bio-based, self-healing, mechanically and chemically recyclable thermosets, starting from photocurable resins, which were further employable in DLP 3D printing processes.

Funding

The work was carried out in the frame of the project "Sustainable – Library of inedited bio-based multicomponent resins for the 3D-printing of self-healing, recyclable thermosets. The project has received funding from the European Union's Horizon 2020 research and innovation programme under the Marie Sklodowska-Curie grant agreement No 101021859 (A.L.), the Knut and Alice Wallenberg Foundation (KAW) through the Wallenberg Wood Science Center (S.S. and M.H.) and the Swedish Research Council, VR (Contract No 2018-03451) (J.Y. and M. H.).

Data Availability

Additional data are available in the supplementary material of this article or from the corresponding author upon reasonable request.

CRediT authorship contribution statement

Anna Liguori: Conceptualization, Data curation, Formal analysis, Visualization, Validation, Funding acquisition, Investigation, Methodology, Writing – original draft. **Sathiyaraj Subramaniyan:** Conceptualization, Writing – review & editing. **Jenevieve G. Yao:** Investigation. **Minna Hakkarainen:** Conceptualization, Data curation, Funding acquisition, Supervision, Validation, Writing – review & editing.

Declaration of Competing Interest

The authors declare that they have no known competing financial interests or personal relationships that could have appeared to influence the work reported in this paper.

Data availability

Data will be made available on request.

Appendix A. Supplementary material

Supplementary data to this article can be found online at https://doi.org/10.1016/j.eurpolymj.2022.111489.

References

[1] Y.H. Jin, Z.P. Lei, P. Taynton, S.F. Huang, W. Zhang, Malleable and recyclable thermosets: the next generation of plastics, Matter 1 (2019) 1456–1493, https://doi.org/10.1016/j.matt.2019.09.004.
[2] Y.H. Zhang, L. Zhang, G.T. Yang, Y.L. Yao, X. Wei, T.C. Pan, J.T. Wu, M.F. Tian, P. G. Yin, Recent advances in recyclable thermosets and thermoset composites based on covalent adaptable networks, J. Mater. Sci. Technol. 92 (2021) 75–87, https://doi.org/10.1016/j.jmst.2021.03.043.
[3] X.W. Xu, S.Q. Ma, H.Z. Feng, J.F. Qiu, S. Wang, Z. Yu, J. Zhu, Dissociate transfer exchange of tandem dynamic bonds endows covalent adaptable networks with fast reprocessability and high performance, Polym. Chem. 12 (2021) 5217–5228, https://doi.org/10.1039/D1PY01045J.
[4] C. Pronoitis, M. Hakkarainen, K. Odelius, Long-chain polyamide covalent adaptable networks based on renewable ethylene brassylate and disulfide exchange, Polym. Chem. 12 (39) (2021) 5668–5678.
[5] S. Huang, X. Kong, Y. Xiong, X. Zhang, H. Chen, W. Jiang, Y. Niu, W. Xu, C. Ren, An overview of dynamic covalent bonds in polymer material and their applications, Eur. Polym. J. 141 (2020), 110094, https://doi.org/10.1016/j.eurpolymj.2020.110094.
[6] A. Martínez-Castañeda, H. Rodríguez-Solla, C. Concellón, V. del Amo, TBD/Al2O3: a novel catalytic system for dynamic intermolecular aldol reactions that exhibit complex system behaviour, Org. Biomol. Chem. 10 (2012) 1976, https://doi.org/10.1039/C2OB06648C.
[7] M. Holler, N. Allenbach, J. Sonet, J.-F. Nierengarten, The high yielding synthesis of pillar[5]arenes under Friedel-Crafts conditions explained by dynamic covalent bond formation, Chem. Commun. 48 (20) (2012) 2576–2578.
[8] P.A. Fernandes, M.J. Ramos, Theoretical insights into the mechanism for thiol/disulfide exchange, Chem. Eur. J. 10 (2004) 257.
[9] A. Liguori, M. Hakkarainen, Designed from biobased materials for recycling: imine-based covalent adaptable networks, Macromol. Rapid Commun. 43 (13) (2022) 2100816.
[10] P. Chakma, D. Konkolewicz, Dynamic covalent bonds in polymeric materials, Angew. Chem. 131 (29) (2019) 9784–9797.
[11] K. Hong, Q.M. Sun, X.Y. Zhang, L.J. Fan, T. Wu, J.Z. Du, Y.Q. Zhu, Fully bio-based high-performance thermosets with closed-loop recyclability, ACS Sustainable Chem. Eng. 10 (2022) 1036–1046, https://doi.org/10.1021/acssuschemeng.1c07523.
[12] J.T. Wan, J.Q. Zhao, X.W. Zhang, H. Fan, J.H. Zhang, D.D. Hu, P.J. Jin, D.Y. Wang, Epoxy thermosets and materials derived from bio-based monomeric phenols: Transformations and performances, Prog. Polym. Sci. 108 (2020), 101287, https://doi.org/10.1016/j.progpolymsci.2020.101287.
[13] R.L. Quirino, K. Monroe, C.H. Fleischer, E. Biswas, M.R. Kessler, Thermosetting polymers from renewable sources, Polym. Int. 70 (2) (2021) 167–180.
[14] J.K. Liu, J.Y. Dai, W.W. Zhao, W.J. Yu, X.Q. Liu, Synthesis of sustainable thermosetting resins: high performance and functionalization, Acta Polym. Sin. 53 (2022) 107–118.
[15] A. Saikia, N. Karak, Renewable resource based thermostable tough hyperbranched epoxy thermosets as sustainable materials, Polym. Degrad. Stab. 135 (2017) 8–17, https://doi.org/10.1016/j.polymdegradstab.2016.11.014.

[16] X.X. Yang, L.Z. Guo, X. Xu, S.B. Shang, H. Liu, A fully bio-based epoxy vitrimer: Self-healing, triple-shape memory and reprocessing triggered by dynamic covalent bond exchange, Mater. Des. 186 (2020), 108248, https://doi.org/10.1016/j.matdes.2019.108248.
[17] W.C. Yuan, S.Q. Ma, S. Wang, Q. Li, B.B. Wang, X.W. Xu, K.F. Huang, J. Chen, S. S. You, J. Zhu, Synthesis of fully bio-based diepoxy monomer with dicyclo diacetal for high-performance, readily degradable thermosets, Eur. Polym. J. 17 (2019) 200–207, https://doi.org/10.1016/j.eurpolymj.2019.05.028.
[18] J.L. Ye, S.Q. Ma, B.B. Wang, Q.M. Chen, K. Huang, X.W. Xu, Q. Li, S. Wang, N. Lu, J. Zhu, High-performance bio-based epoxies from ferulic acid and furfuryl alcohol: synthesis and properties, Green Chem. 23 (2021) 1772–1781, https://doi.org/10.1039/D0GC03946B.
[19] S. Dhers, G. Vantomme, L. Avérous, A fully bio-based polyimine vitrimer derived from fructose, Green Chem. 21 (7) (2019) 1596–1601.
[20] M. Fache, B. Boutevin, S. Caillol, Vanillin, A key-intermediate of biobased polymers, Eur. Polym. J. 68 (2015) 488–502, https://doi.org/10.1016/j.eurpolymj.2015.03.050.
[21] M. Fache, B. Boutevin, S. Caillol, Vanillin production from lignin and its use as a renewable chemical, ACS Sustainable Chem. Eng. 4 (2016) 35–46, https://doi.org/10.1021/acssuschemeng.5b01344.
[22] X. Zhao, Y. Zhang, H. Jiang, H. Zang, Y. Wang, S. Sun, C. Li, Efficient vanillin biosynthesis by recombinant lignin-degrading bacterium Arthrobacter sp. C2 and its environmental profile via life cycle assessment, Bioresour. Technol. 347 (2022), 126434, https://doi.org/10.1016/j.biortech.2021.126434.
[23] M. Fache, E. Darroman, V. Besse, R. Auvergne, S. Caillol, B. Boutevin, Vanillin, a promising biobased building-block for monomer synthesis, Green Chem. 16 (2014) 1987–1998, https://doi.org/10.1039/C3GC42613K.
[24] S. Wang, S. Ma, Q. Li, W. Yuan, B. Wang, J. Zhu, Robust, Fire-Safe, Monomer-Recovery, Highly Malleable Thermosets from Renewable Bioresources, Macromol. 51 (2018) 8001−8012. https://doi.org/10.1021/acs.macromol.8b01601.
[25] H. Memon, Y. Wei, L. Zhang, Q. Jiang, W. Liu, An imine-containing epoxy vitrimer with versatile recyclability and its application in fully recyclable carbon fiber reinforced composites, Compos. Sci. Technol. 199 (2020), 108314, https://doi.org/10.1016/j.compscitech.2020.108314.
[26] Y.-Y. Liu, G.-L. Liu, Y.-D. Li, Y. Weng, J.-B. Zeng, Biobased high-performance epoxy vitrimer with UV shielding for recyclable carbon fiber reinforced composites, ACS Sustain. Chem. Eng. 9 (2021) 4638–4647, https://doi.org/10.1021/acssuschemeng.1c00231.
[27] X. Liu, E. Zhang, Z. Feng, J. Liu, B. Chen, L. Liang, Degradable bio-based epoxy vitrimers based on imine chemistry and their application in recyclable carbon fiber composites, J. Mater. Sci. 56 (2021) 15733–15751, https://doi.org/10.1007/s10853-021-06291-5.
[28] H. Memon, H. Liu, M.A. Rashid, L. Chen, Q. Jiang, L. Zhang, Y. Wei, W. Liu, Y. Qiu, Vanillin-based epoxy vitrimer with high performance and closed-loop recyclability, Macromolecul. 53 (2020) 621–630, https://doi.org/10.1021/acs.macromol.9b02006.
[29] S. Wang, S. Ma, C. Xu, Y. Liu, J. Dai, Z. Wang, X. Liu, J. Chen, X. Shen, J. Wei, J. Zhu, Vanillin-derived high-performance flame retardant epoxy resins: facile synthesis and properties, Macromolecules 50 (2017) 1892–1901, https://doi.org/10.1021/acs.macromol.7b00097.
[30] S. Wang, S. Ma, Q. Li, X. Xu, B. Wang, W. Yuan, S. Zhou, S. You, J. Zhu, Facile in situ preparation of high-performance epoxy vitrimer from renewable resources and its application in nondestructive recyclable carbon fiber composite, Green Chem. 21 (6) (2019) 1484–1497.
[31] X. Xu, S. Ma, J. Wu, J. Yang, B. Wang, S. Wang, Q. Li, J. Feng, S. You, J. Zhu, High-performance, command-degradable, antibacterial Schiff base epoxy thermosets: synthesis and properties, J. Mater. Chem. A 7 (25) (2019) 15420–15431.
[32] S. Zhao, M.M. Abu-Omar, Recyclable and malleable epoxy thermoset bearing aromatic imine bonds, Macromolecules 51 (2018) 9816–9824, https://doi.org/10.1021/acs.macromol.8b01976.
[33] Q. Yu, X. Peng, Y. Wang, H. Geng, A. Xu, X. Zhang, W. Xu, D. Ye, Vanillin-based degradable epoxy vitrimers: reprocessability and mechanical properties study, Eur. Polym. J. 117 (2019) 55–63, https://doi.org/10.1016/j.eurpolymj.2019.04.053.
[34] H. Geng, Y. Wang, Q. Yu, S. Gu, Y. Zhou, W. Xu, X. Zhang, D. Ye, Vanillin-based polyschiff vitrimers: reprocessability and chemical recyclability, ACS Sustainable Chem. Eng. 6 (2018) 15463–15470, https://doi.org/10.1021/acssuschemeng.8b03925.
[35] Z. Zhou, X. Su, J. Liu, R. Liu, Ren Liu, Synthesis of vanillin-based polyimine vitrimers with excellent reprocessability, fast chemical degradability, and adhesion, ACS Appl. Polym. Mater. 2 (12) (2020) 5716–5725.
[36] T. Liu, J. Peng, J. Liu, X. Hao, C. Guo, R. Ou, Z. Liu, Q. Wang, Fully recyclable, flame-retardant and high-performance carbon fiber composites based on vanillin-terminated cyclophosphazene polyimine thermosets, Compos. B 224 (2021), 109188, https://doi.org/10.1016/j.compositesb.2021.109188.
[37] H. Nabipour, H. Niu, X. Wang, S. Batool, Y. Hu, Fully bio-based epoxy resin derived from vanillin with flame retardancy and degradability, React. Funct. Polym. 168 (2021), 105034, https://doi.org/10.1016/j.reactfunctpolym.2021.105034.
[38] X. Su, Z. Zhou, J. Liu, J. Luo, R. Liu, A recyclable vanillin-based epoxy resin with high-performance that can compete with DGEBA, Eur. Polym. J. 140 (2020), 110053, https://doi.org/10.1016/j.eurpolymj.2020.110053.
[39] Y. Xu, K. Odelius, M. Hakkarainen, Photocurable, thermally reprocessable, and chemically recyclable vanillin-based imine thermosets, ACS Sustain. Chem. Eng. 8 (2020) 17272–17279, https://doi.org/10.1021/acssuschemeng.0c06248.
[40] M. Tehfe, F. Louradour, J. Lalevée, J.P. Fouassier, Photopolymerization reactions: on the way to a green and sustainable chemistry, Appl. Sci. 3 (2013) 490–514, https://doi.org/10.3390/app3020490.
[41] S. Dalle Vacche, A. Vitale, R. Bongiovanni, Photocuring of epoxidized cardanol for biobased composites with microfibrillated cellulose, Molecules 24 (2019) 3858, https://doi.org/10.3390/molecules24213858.
[42] M. Degli Esposti, F. Pilati, M. Bondi, S. de Niederhäusern, R. Iseppi, M. Toselli, Maurizio Toselli, Preparation, characterization, and antibacterial activity of photocured thymol-doped acrylic resins, J. Coat. Technol. Res. 10 (3) (2013) 371–379.
[43] J.F. Stanzione III, J.M. Sadler, J.J. La Scala, K.H. Reno, R.P. Wool, Vanillin-based resin for use in composite applications, Green Chem. 14 (2012) 2346–2352, https://doi.org/10.1039/C2GC35672D.
[44] X. Li, X. Wang, S. Subramaniyan, Y. Liu, J. Rao, B. Zhang, Hyperbranched polyesters based on indole- and lignin-derived monomeric aromatic aldehydes as effective nonionic antimicrobial coatings with excellent biocompatibility, Biomacromolecules 23 (2022) 150–162, https://doi.org/10.1021/acs.biomac.1c01186.
[45] L. Wang, Y. Wang, L. Ren, Synthesis and characterization of novel biodegradable aromatic-aliphatic poly(ester amide)s containing ethylene oxide moieties, J. Appl. Polym. Sci. 109 (2008) 1310–1318, https://doi.org/10.1002/app.28103.
[46] B. Wang, Y. Zhang, P. Song, Z. Guo, J. Cheng, Z. Fang, Biodegradable aliphatic/aromatic copolyesters based onterephthalic acid and poly(l-lactic acid): synthesis, characterization and hydrolytic degradation, Chin. J. Polym. Sci. 28 (2010) 405–415, https://doi.org/10.1007/s10118-010-9032-y.
[47] Y. Sun, D. Sheng, H. Wu, X. Tian, H. Xie, B. Shi, X. Liu, Y. Yang, Bio-based vitrimer-like polyurethane based on dynamic imine bond with high-strength, reprocessability, rapid-degradability and antibacterial ability, Polymer 233 (2021), 124208, https://doi.org/10.1016/j.polymer.2021.124208.
[48] F. Song, Z. Li, P. Jia, M. Zhang, C. Bo, G. Feng, L. Hu, Y. Zhou, Tunable “soft and stiff”, self-healing, recyclable, thermadapt shape memory biomass polymers based on multiple hydrogen bonds and dynamic imine bonds, J. Mater. Chem. A 7 (21) (2019) 13400–13410.
[49] X.L. Zhao, Y.Y. Liu, Y. Weng, Y.D. Li, J.B. Zeng, Sustainable epoxy vitrimers from epoxidized soybean oil and vanillin, ACS Sustain. Chem. Eng. 8 (2020) 15020–15029, https://doi.org/10.1021/acssuschemeng.0c05727.
[50] E. Desnoes, L. Toubal, A.H. Bouazza, D. Montplaisir, Biosourced vanillin Schiff base platform monomers as substitutes for DGEBA in thermoset epoxy, Polym. Eng. Sci. 60 (2020) 2593–2605, https://doi.org/10.1002/pen.25497.
[51] M. Lebedevaite, V. Talacka, J. Ostrauskaite, High biorenewable content acrylate photocurable resins for DLP 3D printing, J. Appl. Polym. Sci. 138 (2021) 138: e50233, https://doi.org/10.1002/app.50233.
[52] C. Noè, A. Cosola, C. Tonda-Turo, R. Sesana, C. Delprete, A. Chiappone, M. Hakkarainen, M. Sangermano, DLP-printable fully biobased soybean oil composites, Polymer 247 (2022) 124779.
[53] E.M. Maines, M.K. Porwal, C.J. Ellison, T.M. Reineke, Sustainable advances in SLA/DLP 3D printing materials and processes, Green Chem. 23 (18) (2021) 6863–6897.
[54] J.T. Miao, M. Ge, S. Peng, J. Zhong, Y. Li, Z. Weng, L. Wu, L. Zheng, Dynamic imine bond-based shape memory polymers with permanent shape reconfigurability for 4D printing, ACS Appl. Mater. Interfaces 11 (2019) 40642–40651, https://doi.org/10.1021/acsami.9b14145.